AIMS Mathematics, 7(9): 17252–17268.
DOI:10.3934/math.2022950
Received: 23 May 2022
Revised: 29 June 2022
Accepted: 07 July 2022
Published: 25 July 2022

http://www.aimspress.com/journal/Math

Research article

A novel finite difference based numerical approach for Modified Atangana-Baleanu Caputo derivative

Reetika Chawla[1], **Komal Deswal**[1,*], **Devendra Kumar**[1] **and Dumitru Baleanu**[2,3]

[1] Department of Mathematics, Birla Institute of Technology and Science, Pilani, Rajasthan-333031, India

[2] Department of Mathematics and Computer Sciences, Faculty of Arts and Sciences, Cankaya University, Ankara 06530, Turkey

[3] Institute of Space Science, Magurle-Bucharest 077125, Romania

* **Correspondence:** Email: komaldeswal94@gmail.com.

Abstract: In this paper, a new approach is presented to investigate the time-fractional advection-dispersion equation that is extensively used to study transport processes. The present modified fractional derivative operator based on Atangana-Baleanu's definition of a derivative in the Caputo sense involves singular and non-local kernels. A numerical approximation of this new modified fractional operator is provided and applied to an advection-dispersion equation. Through Fourier analysis, it has been proved that the proposed scheme is unconditionally stable. Numerical examples are solved that validate the theoretical results presented in this paper and ensure the proficiency of the numerical scheme.

Keywords: fractional derivative; advection dispersion equation; finite difference method
Mathematics Subject Classification: 26A33, 35R11, 65M06, 65M12, 65N22

1. Introduction

In the field of fractional calculus, fractional derivatives play a very important role in explaining the complex processes in applied sciences and engineering [1, 2]. Anomalous dispersion processes are widely studied using fractional derivatives in areas like electron transportation [3], turbulence [4] and dissipation [5]. Such a process reveals the striking properties of long-range interaction that cannot be well demonstrated by using standard integer-order differential equations. So, the fractional derivatives are used to describe such anomalous behavior in various processes [6]. Some fractional derivatives like the Grunwald-Letnikov fractional derivative, Riemann-Liouville (RL) derivative and Caputo derivative have been studied numerically and theoretically for various fractional differential

equations. Many researchers have extensively used these operators for solving fractional differential equations, as broadly explained in [7–10] and references therein. Later, it was shown in [11] that the solutions of time-fractional differential equations that were analyzed using the RL or Caputo derivative exhibit weak singularities at the initial time $t = 0$ that can be resolved, as some authors have shown by introducing the fractional derivatives involving non-singular kernels. In 2015, a fractional derivative was introduced, named the Caputo-Fabrizio fractional derivative by Caputo and Fabrizio [12]. This fractional derivative involves a non-singular kernel which can describe the material heterogeneities and fluctuations with different scales. Some authors have solved the fractional differential equations using the Caputo-Fabrizio definition [13–15]. After that, in 2016, we studied a new type of fractional derivative, called the Atangana-Baleanu Caputo (ABC) derivative that also involves the non-singular kernel and generalizes the Caputo-Fabrizio definition [16]. Some recent work that has been done by researchers who have used the ABC derivative to solve fractional differential equations is given in [17–19].

Recently, Refai and Baleanu [20] introduced a modification of the ABC fractional differential operator, called the Modified Atangana-Baleanu Caputo (MABC) derivative, which is an extension of the ABC derivative to a wider space, and demonstrated that there are numerous fractional differential equations that can be solved by using the MABC derivative that cannot be solved with the ABC derivative. Therefore, in this article, we present a novel finite difference discrete scheme that modifies the ABC derivative; the related fractional differential equations can be easily initialized using this modified operator. This modified fractional operator, also called the MABC-derivative, has the integrable singularity at the origin [20]. The present numerical method in which the time-fractional derivative is considered to be an MABC-derivative can be applied to solve various models. Here, we have considered an example of the time-fractional advection-dispersion equation that is used to model the transport of passive tracers that are carried by fluid in a heterogeneous medium [21–23].

The paper is organized in the following way. In Section 2, a few definitions of fractional calculus are presented. The crucial part of the paper is presented in Section 3, which involves a numerical approximation of the MABC derivative, estimation of the truncation error and evaluation of the numerical solution of the time fractional advection-dispersion equation. In Section 4, the stability of the numerical scheme is presented through the use of Fourier analysis. In Section 5, some numerical examples are tested using the numerical plots and tabulated results to verify the theoretical results. At last, we conclude the paper in Section 6.

2. Preliminaries

Some basic definitions of fractional calculus are covered in this section, additional information on the subject can be found in [2, 16, 20, 24, 25].

- The RL fractional derivative (of order $\alpha \in R$) of a function f is defined as

$$ {}_0D_t^{\alpha} f(t) = \frac{1}{\Gamma(r-\alpha)} \frac{d^r}{dt^r} \int_0^t (t-s)^{r-\alpha-1} f(s)\, ds, \ t > 0, \tag{2.1} $$

  where r is a positive integer and $r - 1 < \alpha < r$.

- The Caputo fractional derivative (of order $\alpha \in R$) of a function f is defined as

$$ {}_0^C D_t^\alpha f(t) = \frac{1}{\Gamma(r-\alpha)} \int_0^t (t-s)^{r-\alpha-1} f^{(r)}(s)\, ds,\ t > 0, \tag{2.2} $$

  where r is a positive integer and $r - 1 \leq \alpha < r$.
- The ABC derivative of order $0 < \alpha < 1$ of a function $f \in H^1(0,1)$ is defined as

$$ {}_0^{ABC} D_t^\alpha f(t) = \frac{\Re(\alpha)}{1-\alpha} \int_0^t f'(s) E_{\alpha,1}\left[\frac{-\alpha}{1-\alpha}(t-s)^\alpha\right] ds, \tag{2.3} $$

  where $\Re(\alpha)$ is a normalization function obeying $\Re(0) = \Re(1) = 1$, and the Mittag-Leffler function is defined as

$$ E_{\alpha,\beta}(z) = \sum_{r=0}^{\infty} \frac{z^r}{\Gamma(\alpha r + \beta)}. \tag{2.4} $$

- The MABC derivative of order $0 < \alpha < 1$ of a function $f \in L^1(0,1)$ in the Caputo sense is defined as

$$ {}_0^{MABC} D_t^\alpha f(t) = \frac{\Re(\alpha)}{1-\alpha}\left[f(t) - E_\alpha(-\mu_\alpha t^\alpha) f(0) - \mu_\alpha \int_0^t (t-s)^{\alpha-1} E_{\alpha,\alpha}[-\mu_\alpha (t-s)^\alpha] f(s)\, ds\right], \tag{2.5} $$

  where $\mu_\alpha = \frac{\alpha}{1-\alpha}$.

The fractional derivatives are widely used to study the memory effect in the complex processes which is well described by kernels (singular and non-singular). The MABC fractional derivative that modifies the ABC fractional derivative involves the kernel that has integrable singularity at the origin, which leads to new solutions of several fractional differential equations and a description of the dynamics of complex processes that is better than the ABC fractional derivative. For more information, refer to [20]. We now numerically formulate the MABC derivative that helps to solve the fractional differential equations.

3. Numerical scheme formulation using the MABC derivative

In this article, we formulate the time fractional advection dispersion equation in which the derivative in time is considered as the MABC derivative.

$$ {}_0^{MABC} D_t^\alpha u = \nu \frac{\partial^2 u}{\partial x^2} - \rho \frac{\partial u}{\partial x} + f(x,t), \quad 0 < x < L, \quad 0 < t \leq T, \tag{3.1a} $$

with the initial condition

$$ u(x,0) = \phi_0(x),\ 0 \leq x \leq L, \tag{3.1b} $$

and the boundary conditions

$$ u(0,t) = u(L,t) = 0,\ 0 \leq t \leq T. \tag{3.1c} $$

Here, we consider that ν and ρ are the constants.

To discretize Eq (3.1a), we begin with an equidistant mesh $t_k = k\tau,\ k = 0, 1, 2, \ldots, M_t$ and $x_n = nh,\ n = 0, 1, 2, \ldots, N_x$, with the step size $h = L/N_x$ in both the temporal and spatial directions, where $\tau = T/M_t$ and M_t, N_x are the number of partitions of the temporal domain $[0, T]$ and spatial domain $[0, L]$, respectively.

3.1. Time discretization using the MABC derivative

Using the definition given by Eq (2.5) and applying the Taylor series expansion to discretize the function $f(t)$, we get

$$\begin{aligned} f(t) &= f(t_q) + (t-t_q)f'(t_q) + \frac{(t-t_q)^2}{2}f''(t_q) + O((t-t_q)^3), \\ &= f(t_q) + (t-t_q)\frac{f(t_{q+1}) - f(t_{q-1})}{2\tau} - \frac{f^{(3)}(t_q)}{3!}(t-t_q)\tau^2 + O((t-t_q)^2), \quad t \in (t_q, t_{q+1}). \end{aligned} \tag{3.2}$$

Since,

$$f'(t_q) = \frac{f(t_{q+1}) - f(t_{q-1})}{2\tau} - \frac{f^{(3)}(t_q)}{3!}\tau^2 + O(\tau^4), \quad t \in (t_q, t_{q+1}),$$

We have that

$$\begin{aligned} {}^{MABC}_{0}D^{\alpha}_{t} f(t)|_{t=t_k} &= \frac{\mathfrak{N}(\alpha)}{1-\alpha}\Bigg[f(t_k) - E_\alpha(-\mu_\alpha t_k^\alpha)f(0) \\ &\quad - \mu_\alpha \sum_{q=0}^{k-1}\int_{t_q}^{t_{q+1}} (t_k - s)^{\alpha-1} E_{\alpha,\alpha}[-\mu_\alpha(t_k-s)^\alpha]\left(f(t_q) + (s-t_q)\frac{f(t_{q+1}) - f(t_{q-1})}{2\tau}\right)ds\Bigg] + R_k \\ &= \frac{\mathfrak{N}(\alpha)}{1-\alpha}\Bigg[f(t_k) - E_\alpha(-\mu_\alpha t_k^\alpha)f(0)\Bigg] - \frac{\mathfrak{N}(\alpha)}{1-\alpha}\mu_\alpha \sum_{q=0}^{k-1}\int_{t_q}^{t_{q+1}} (t_k-s)^{\alpha-1}E_{\alpha,\alpha}[-\mu_\alpha(t_k-s)^\alpha]f(t_q)ds \\ &\quad - \frac{\mathfrak{N}(\alpha)}{1-\alpha}\mu_\alpha \sum_{q=0}^{k-1}\int_{t_q}^{t_{q+1}} (t_k-s)^{\alpha-1}E_{\alpha,\alpha}[-\mu_\alpha(t_k-s)^\alpha](s-t_q)\frac{f(t_{q+1}) - f(t_{q-1})}{2\tau}ds + R_k. \end{aligned}$$

Now for simplification we consider that

$$\begin{aligned} A &= \sum_{q=0}^{k-1}\int_{t_q}^{t_{q+1}} (t_k-s)^{\alpha-1}E_{\alpha,\alpha}[-\mu_\alpha(t_k-s)^\alpha]f(t_q)ds, \\ B &= \sum_{q=0}^{k-1}\int_{t_q}^{t_{q+1}} (t_k-s)^{\alpha-1}E_{\alpha,\alpha}[-\mu_\alpha(t_k-s)^\alpha](s-t_q)\frac{f(t_{q+1}) - f(t_{q-1})}{2\tau}ds. \end{aligned}$$

Now, A and B can be evaluated using the definition of the Mittag-Leffler function, as follows:

$$\begin{aligned} A &= \sum_{q=0}^{k-1}\int_{t_q}^{t_{q+1}} (t_k-s)^{\alpha-1}E_{\alpha,\alpha}[-\mu_\alpha(t_k-s)^\alpha]f(t_q)ds \\ &= \sum_{q=0}^{k-1} f(t_q)[(t_k-t_q)^\alpha E_{\alpha,\alpha+1}(-\mu_\alpha(t_k-t_q)^\alpha) - (t_k-t_{q+1})^\alpha E_{\alpha,\alpha+1}(-\mu_\alpha(t_k-t_{q+1})^\alpha)], \end{aligned} \tag{3.3}$$

$$B = \sum_{q=0}^{k-1}\int_{t_q}^{t_{q+1}} (t_k-s)^{\alpha-1}E_{\alpha,\alpha}[-\mu_\alpha(t_k-s)^\alpha](s-t_q)\frac{f(t_{q+1}) - f(t_{q-1})}{2\tau}ds$$

$$= \sum_{q=0}^{k-1} \Big(\frac{f(t_{q+1}) - f(t_{q-1})}{2\tau}\Big)\Big[- (t_k - t_{q+1})^{\alpha}\tau E_{\alpha,\alpha+1}(-\mu_\alpha(t_k - t_{q+1})^{\alpha})$$

$$- (t_k - t_{q+1})^{\alpha+1} E_{\alpha,\alpha+2}(-\mu_\alpha(t_k - t_{q+1})^{\alpha}) + (t_k - t_q)^{\alpha+1} E_{\alpha,\alpha+2}(-\mu_\alpha(t_k - t_q)^{\alpha})\Big]. \tag{3.4}$$

After simplifying, we obtain

$${}^{MABC}_{0}D_t^{\alpha} f(t)|_{t=t_k} = \frac{\mathfrak{N}(\alpha)}{1-\alpha}\Big[f(t_k) - E_\alpha(-\mu_\alpha t_k^{\alpha}) f(0)\Big] - \sum_{q=0}^{k-1}[C_q^k f(t_{q-1}) + D_q^k f(t_q) + F_q^k f(t_{q+1})] + R_k, \tag{3.5}$$

where

$$\begin{aligned}
C_q^k &= -\frac{\mathfrak{N}(\alpha)}{1-\alpha}\frac{\mu_\alpha \tau^{\alpha}}{2}\{-(k-q-1)^{\alpha}\ {}_1E_{q+1}^k - (k-q-1)^{\alpha+1}\ {}_2E_{q+1}^k + (k-q)^{\alpha+1}\ {}_2E_q^k\},\\
D_q^k &= \frac{\mathfrak{N}(\alpha)\mu_\alpha \tau^{\alpha}}{(1-\alpha)}\{(k-q)^{\alpha}\ {}_1E_q^k - (k-q-1)^{\alpha}\ {}_1E_{q+1}^k\},\\
F_q^k &= -C_q^k,
\end{aligned} \tag{3.6}$$

where $E_{\alpha,\alpha+1}[-\mu_\alpha(t_k - t_q)^{\alpha}]$ and $E_{\alpha,\alpha+2}[-\mu_\alpha(t_k - t_q)^{\alpha}]$ are respectively represented as ${}_1E_q^k$ and ${}_2E_q^k$.

The truncation error R_k is given as

$$\begin{aligned}
R_k &= \frac{\mathfrak{N}(\alpha)}{1-\alpha}\mu_\alpha \sum_{q=0}^{k-1}\int_{t_q}^{t_{q+1}} \Big[- \frac{f^{(3)}(t_q)}{3!}(s-t_q)\tau^2\Big](t_k - s)^{\alpha-1} E_{\alpha,\alpha}[-\mu_\alpha(t_k - s)^{\alpha}] f(s)\, ds\\
&= -\frac{\mathfrak{N}(\alpha)}{1-\alpha}\mu_\alpha \sum_{q=0}^{k-1}\int_{t_q}^{t_{q+1}} \Big[\frac{f^{(3)}(t_q)}{3!}(s-t_q)\tau^2\Big](t_k - s)^{\alpha-1} E_{\alpha,\alpha}[-\mu_\alpha(t_k - s)^{\alpha}] f(s)\, ds\\
&= -\frac{\mathfrak{N}(\alpha)}{1-\alpha}\mu_\alpha \sum_{q=0}^{k-1}\frac{f^{(3)}(t_q)}{3!}\tau^2\int_{t_q}^{t_{q+1}} (s-t_q)(t_k - s)^{\alpha-1} E_{\alpha,\alpha}[-\mu_\alpha(t_k - s)^{\alpha}] f(s)\, ds\\
&= -\frac{\mathfrak{N}(\alpha)}{1-\alpha}\mu_\alpha \sum_{q=0}^{k-1}\frac{f^{(3)}(t_q)}{3!}\tau^2\Bigg(\Big[- (s-t_q)(t_k - s)^{\alpha} E_{\alpha,\alpha+1}[-\mu_\alpha(t_k - s)^{\alpha}]\Big]_{t_q}^{t_{q+1}}\\
&- \Big[(t_k - s)^{\alpha+1} E_{\alpha,\alpha+2}[-\mu_\alpha(t_k - s)^{\alpha}]\Big]_{t_q}^{t_{q+1}}\Bigg)\\
&= -\frac{\mathfrak{N}(\alpha)}{1-\alpha}\mu_\alpha \sum_{q=0}^{k-1}\frac{f^{(3)}(t_q)}{3!}\tau^2\Bigg(- (t_{q+1} - t_q)(t_k - t_{q+1})^{\alpha} E_{\alpha,\alpha+1}[-\mu_\alpha(t_k - t_{q+1})^{\alpha}]\\
&- (t_k - t_{q+1})^{\alpha+1} E_{\alpha,\alpha+2}[-\mu_\alpha(t_k - t_{q+1})^{\alpha}] + (t_k - t_q)^{\alpha+1} E_{\alpha,\alpha+2}[-\mu_\alpha(t_k - t_q)^{\alpha}]\Bigg).
\end{aligned}$$

Thus, we obtain the following equation at the $k = M_t$ time step

$$\begin{aligned}
R_k &= -\frac{\mathfrak{N}(\alpha)}{1-\alpha}\mu_\alpha \frac{f^{(3)}(t_0)}{3!}\tau^2\Bigg(- (t_1 - t_0)(t_{M_t} - t_1)^{\alpha} E_{\alpha,\alpha+1}[-\mu_\alpha(t_{M_t} - t_1)^{\alpha}]\\
&- (t_{M_t} - t_1)^{\alpha+1} E_{\alpha,\alpha+2}[-\mu_\alpha(t_{M_t} - t_1)^{\alpha}] + (t_{M_t} - t_0)^{\alpha+1} E_{\alpha,\alpha+2}[-\mu_\alpha(t_{M_t} - t_0)^{\alpha}]\Bigg) + \ldots
\end{aligned}$$

$$= -\frac{\mathfrak{N}(\alpha)}{1-\alpha}\mu_\alpha \frac{f^{(3)}(t_0)}{3!}\tau^2\Big(-(\tau)((M_t-1)\tau)^\alpha E_{\alpha,\alpha+1}[-\mu_\alpha((M_t-1)\tau)^\alpha]$$

$$-((M_t-1)\tau)^{\alpha+1}E_{\alpha,\alpha+2}[-\mu_\alpha(t_{M_t}-t_1)^\alpha] + (M_t\tau)^{\alpha+1}E_{\alpha,\alpha+2}[-\mu_\alpha(t_{M_t}-t_0)^\alpha]\Big) + \dots$$

Using the fact that $M_t\tau = T$ which is a constant, we obtain the global truncation error

$$|R_k| \le C\frac{\mathfrak{N}(\alpha)}{1-\alpha}\mu_\alpha \max_{0\le q\le M_t-1}\Big|\frac{f^{(3)}(t_q)}{3!}\Big|\tau^2,$$

where C is a constant.

3.2. Spatial discretization

The first- and second-order spatial derivatives can be approximated using the following finite-difference formulas:

$$\begin{aligned}\frac{\partial u(x_n,t_k)}{\partial x} &= \frac{u^k_{n+1}-u^k_{n-1}}{2h} + O(h^2),\\ \frac{\partial^2 u(x_n,t_k)}{\partial x^2} &= \frac{u^k_{n+1}-2u^k_n+u^k_{n-1}}{h^2} + O(h^2),\end{aligned} \tag{3.7}$$

for $0 \le n \le N_x$ and $1 \le k \le M_t$.

3.3. MABC application: Advection-dispersion equation

The fully discretized numerical scheme for Eq (3.1), following the discretization in the temporal and spatial directions at (x_n, t_k) is presented in the following way using Eqs (3.5) and (3.7)

$$\frac{\mathfrak{N}(\alpha)}{1-\alpha}\Big[u^k_n - E_\alpha(-\mu_\alpha t_k^\alpha)u^0_n\Big] - \sum_{q=0}^{k-1}[C^k_q u^{q-1}_n + D^k_q u^q_n + F^k_q u^{q+1}_n] = \frac{\nu}{h^2}(u^k_{n-1}-2u^k_n+u^k_{n+1})$$

$$-\frac{\rho}{2h}(u^k_{n+1}-u^k_{n-1}) + f(x_n,t_k) + O(\tau^2+h^2), \tag{3.8}$$

with the initial and boundary conditions given as

$$\begin{aligned}u^0_n &= \phi_0(x_n),\ 0 \le n \le N_x,\\ u^k_0 &= u^k_{N_x} = 0,\ 0 \le k \le M_t.\end{aligned}$$

The numerical scheme at different time levels is presented as follows

For $k = 1$,

$$\Big(-\frac{\nu}{h^2}-\frac{\rho}{2h}\Big)u^1_{n-1} + \Big(\frac{\mathfrak{N}(\alpha)}{1-\alpha} - F^1_0 + \frac{2\nu}{h^2}\Big)u^1_n + \Big(-\frac{\nu}{h^2}+\frac{\rho}{2h}\Big)u^1_{n+1} = (C^1_0+D^1_0)u^0_n$$

$$+\frac{\mathfrak{N}(\alpha)}{1-\alpha}E_\alpha(-\mu_\alpha t_1^\alpha)u^0_n + f(x_n,t_1), \tag{3.9}$$

for $k = 2$,

$$\Big(-\frac{\nu}{h^2}-\frac{\rho}{2h}\Big)u_{n-1}^2+\Big(\frac{\Re(\alpha)}{1-\alpha}-F_1^2+\frac{2\nu}{h^2}\Big)u_n^2+\Big(-\frac{\nu}{h^2}+\frac{\rho}{2h}\Big)u_{n+1}^2=(C_0^2+D_0^2+C_1^2)u_n^0 + (F_0^2+D_1^2)u_n^1+\frac{\Re(\alpha)}{1-\alpha}E_\alpha(-\mu_\alpha t_2^\alpha)u_n^0+f(x_n,t_2), \tag{3.10}$$

for $2 < k \le M_t$,

$$\Big(-\frac{\nu}{h^2}-\frac{\rho}{2h}\Big)u_{n-1}^k+\Big(\frac{\Re(\alpha)}{1-\alpha}-F_{k-1}^k+\frac{2\nu}{h^2}\Big)u_n^k+\Big(-\frac{\nu}{h^2}+\frac{\rho}{2h}\Big)u_{n+1}^k=\sum_{q=1}^{k-2}(C_q^k u_n^{q-1}+D_q^k u_n^q+F_q^k u_n^{q+1}) + C_{k-1}^k u_n^{k-2}+D_{k-1}^k u_n^{k-1}+(C_0^k+D_0^k)u_n^0+F_0^k u_n^1+\frac{\Re(\alpha)}{1-\alpha}E_\alpha(-\mu_\alpha t_k^\alpha)u_n^0+f(x_n,t_k); \tag{3.11}$$

although these apply as $u_n^{-1} = u_n^0 - \tau\frac{\partial u_n^0}{\partial t}+\frac{\tau^2}{2}\frac{\partial^2 u_n^0}{\partial t^2}+O(\tau^3)$, here, we consider the case where $\frac{\partial u(x,0)}{\partial t} = \frac{\partial^2 u(x,0)}{\partial t^2} = 0$, so $u_n^{-1} = u_n^0$.

Using Eqs (3.9)–(3.11) we can express the numerical scheme in the following matrix form:

$$\mathcal{P}^k U^k = \mathcal{Q}^k + \mathcal{R}^k + \mathcal{S}^k, \tag{3.12}$$

where,

$$\mathcal{P}^k = tri\Big[-\frac{\nu}{h^2}-\frac{\rho}{2h},\ \frac{\Re(\alpha)}{1-\alpha}-F_{k-1}^k+\frac{2\nu}{h^2},\ -\frac{\nu}{h^2}+\frac{\rho}{2h}\Big],\ 1\le k\le M_t, \tag{3.13}$$

$$\mathcal{Q}^k=\begin{cases}(C_0^1+D_0^1+\vartheta^1)U^0, & k=1,\\ (C_0^2+D_0^2+C_1^2+\vartheta^2)U^0+(F_0^2+D_1^2)U^1, & k=2,\\ \sum_{q=1}^{k-2}(C_q^k u_n^{q-1}+D_q^k u_n^q+F_q^k u_n^{q+1}) & \\ +C_{k-1}^k u_n^{k-2}+D_{k-1}^k u_n^{k-1}+(C_0^k+D_0^k+\vartheta^k)u_n^0+F_0^k u_n^1, & 2<k\le M_t.\end{cases}$$

$$\begin{aligned}\vartheta^k &= \frac{\Re(\alpha)}{1-\alpha}E_\alpha(-\mu_\alpha t_k^\alpha),\\ U^k &= [u_1^k,\dots,u_n^k,\dots,u_{N_x-1}^k]^T,\\ \mathcal{R}^k &= \Big[\Big(\frac{\nu}{h^2}+\frac{\rho}{2h}\Big)u_0^k,\dots,\Big(\frac{\nu}{h^2}-\frac{\rho}{2h}\Big)u_{N_x}^k\Big]^T,\\ \mathcal{S}^k &= [f_1^k,\dots,f_n^k,\dots,f_{N_x-1}^k]^T.\end{aligned} \tag{3.14}$$

4. Stability analysis

Let the solution U_n^k, $n = 0,1,2,\dots,N_x$, $k = 0,1,2,\dots,M_t$, be an approximation of the equation given by (3.9), and the truncation error is defined as $\epsilon_n^k = u_n^k - U_n^k$. Since Eq (3.9) is satisfied by the approximate solution, by considering the error equation after substituting ϵ_n^k, we obtain the following for $k = 1,2$

$$\mathfrak{a}_1\epsilon_{n-1}^1+\mathfrak{b}_1\epsilon_n^1+\mathfrak{c}_1\epsilon_{n+1}^1=(C_0^1+D_0^1+\vartheta^1)\epsilon_n^0, \tag{4.1}$$

$$\mathfrak{a}_2\epsilon_{n-1}^2 + \mathfrak{b}_2\epsilon_n^2 + \mathfrak{c}_2\epsilon_{n+1}^2 = (C_0^2 + D_0^2 + C_1^2 + \vartheta^2)\epsilon_n^0 + (F_0^2 + D_1^2)\epsilon_n^1, \tag{4.2}$$

and for $k > 2$

$$\begin{aligned}\mathfrak{a}_k\epsilon_{n-1}^k + \mathfrak{b}_k\epsilon_n^k + \mathfrak{c}_k\epsilon_{n+1}^k = &\sum_{q=1}^{k-2}(C_q^k\epsilon_n^{q-1} + D_q^k\epsilon_n^q + F_q^k\epsilon_n^{q+1}) + C_{k-1}^k\epsilon_n^{k-2} + D_{k-1}^k\epsilon_n^{k-1} \\ &+ (C_0^k + D_0^k + \vartheta^k)\epsilon_n^0 + F_0^k\epsilon_n^1,\end{aligned} \tag{4.3}$$

where $\mathfrak{a}_k = -\frac{\nu}{h^2} - \frac{\rho}{2h}$, $\mathfrak{b}_k = \frac{\Re(\alpha)}{1-\alpha} - F_{k-1}^k + \frac{2\nu}{h^2}$, and $\mathfrak{c}_k = -\frac{\nu}{h^2} + \frac{\rho}{2h}$, for all $k = 1, 2, \ldots, M_t$. Consider the grid function

$$\epsilon^k(x) = \begin{cases} 0, & 0 \le x \le x_{\frac{1}{2}}, \\ \epsilon_n^k, & x_{n-\frac{1}{2}} \le x \le x_{n+\frac{1}{2}}, \quad 1 \le n \le N_x - 1, \\ 0, & x_{N_x-\frac{1}{2}} \le x \le x_{N_x}, \end{cases}$$

which has the following Fourier series expansion

$$\epsilon^k(x) = \sum_{l=-\infty}^{\infty} \eta_k(l) e^{\frac{i2\pi lx}{L}}, \quad k = 1, 2, \ldots, M_t,$$

where

$$\eta_k(l) = \frac{1}{L}\int_0^L \epsilon^k(\zeta) e^{\frac{-i2\pi l\zeta}{L}} d\zeta,$$

represents the discrete Fourier coefficients. Introducing the Parseval's identity (for the discrete Fourier transform)

$$\int_0^L |\epsilon^k(x)|^2 dx = \sum_{l=-\infty}^{\infty} |\eta_k(l)|^2,$$

and the norm

$$\|\epsilon^k\|_2 = \left(\sum_{n=1}^{N_x-1} h|\epsilon_n^k|^2\right)^{\frac{1}{2}} = \left(\int_0^L |\epsilon_n^k|^2 dx\right)^{\frac{1}{2}},$$

gives

$$\|\epsilon^k\|_2^2 = \sum_{l=-\infty}^{\infty} |\eta_k(l)|^2.$$

Based on the above analysis, the solution of Eqs (4.1)–(4.3) takes the form $\epsilon_n^k = \eta_k e^{i\beta nh}$, where $\beta = 2\pi l/L$; after simplifying the equations we obtain the following inequalities at different time levels. Now, for $k = 1$, Eq (4.1) yields

$$(\mathfrak{a}_1 e^{-i\beta h} + \mathfrak{b}_1 + \mathfrak{c}_1 e^{i\beta h})\eta_1 = (C_0^1 + D_0^1 + \vartheta^1)\eta_0.$$

Taking the modulus on both sides, we obtain

$$|((\mathfrak{a}_1 + \mathfrak{c}_1)\cos(\beta h) + i(-\mathfrak{a}_1 + \mathfrak{c}_1)\sin(\beta h) + \mathfrak{b}_1)\eta_1| \le |(C_0^1 + D_0^1 + \vartheta^1)\|\eta_0|$$

which implies

$$|\eta_1| \leq \frac{|(C_0^1 + D_0^1 + \vartheta^1)|}{\left|\frac{2\nu}{h^2}(1-\cos(\beta h)) + \frac{\Re(\alpha)}{1-\alpha} - F_0^1 + i\frac{\rho\sin(\beta h)}{h}\right|}|\eta_0|.$$

As h and τ approach zero, we obtain the condition $|\eta_1| \leq |\eta_0|$.

Using the inequality obtained for $k = 1$ and applying the same procedure we get the following inequality for $k = 2$:

$$|\eta_2| \leq \frac{|(C_0^2 + D_0^2 + C_1^2 + \vartheta^2) + (F_0^2 + D_1^2)|}{\left|\frac{2\nu}{h^2}(1-\cos(\beta h)) + \frac{\Re(\alpha)}{1-\alpha} - F_1^2 + i\frac{\rho\sin(\beta h)}{h}\right|}|\eta_0|;$$

thus, we get that $|\eta_2| \leq |\eta_0|$ as $\tau \to 0$. Now, we assume that the inequality holds for $m = 3, \ldots, k-1$ that is

$$|\eta_m| \leq |\eta_0|, \tag{4.4}$$

and we will further prove the same for $m = k$; from Eqs (4.3) and (4.4) we obtain the

$$\begin{aligned}
|\eta_k| &\leq \frac{|\sum_{q=1}^{k-2}(C_q^k + D_q^k + F_q^k) + C_{k-1}^k + D_{k-1}^k + (C_0^k + D_0^k + \vartheta^k) + F_0^k|}{|(\mathfrak{a}_k + \mathfrak{c}_k)\cos(\beta h) + i(-\mathfrak{a}_k + \mathfrak{c}_k)\sin(\beta h) + \mathfrak{b}_k|}|\eta_0| \\
&\leq \frac{|\sum_{q=1}^{k-2} D_q^k + C_{k-1}^k + D_{k-1}^k + (D_0^k + \vartheta^k)|}{\left|\frac{2\nu}{h^2}(1-\cos(\beta h)) + \frac{\Re(\alpha)}{1-\alpha} - F_{k-1}^k + i\frac{\rho\sin(\beta h)}{h}\right|}|\eta_0|. \qquad \text{[from Eq (3.6)]}
\end{aligned}$$

It is clear from previous analysis that as $h, \tau \to 0$, $|\eta_k| \leq |\eta_0|$, which implies $|\epsilon_k| \leq |\epsilon_0|$, $\forall\, k = 1, 2, \ldots, M_t$; thus, we prove, by following the process of mathematical induction, that the numerical scheme is unconditionally stable.

5. Numerical illustrations

In this section, to demonstrate the efficiency and viability of the scheme and validate the computational algorithm and theoretical findings, we consider a test example; the aim was to solve them using MATLAB R2021b. The L_2-norm and relative error measures are defined as

$$E_2^{N_x,M_t} = \|U - u\|_2 = \max_{0\leq k\leq M_t} \sqrt{h\sum_{n=0}^{N_x} |U(x_n, t_k) - u_n^k|^2},$$

and

$$E_R^{N_x,M_t} = \frac{|U(x_n, t_k) - u_n^k|}{|u_n^k|},$$

respectively. Moreover, to show the high precision achieved by the numerical scheme, we compute the order of convergence, ord^{N_x,M_t}, using the formula

$$\text{ord}^{N_x,M_t} = \frac{\ln(\mathrm{E}_2^{N_x,M_t}/\mathrm{E}_2^{2N_x,2M_t})}{\ln 2}.$$

To prove the proficiency of the proposed numerical scheme, the results have been compiled to present in the form of tables and graphs. All graphs were drawn by taking $N_x = M_t = 64$, and all tables were prepared by taking $N_x = M_t$. In Example 5.1, we solve the considered problem in the computational domain $[0, 1]$ with $T = 1$ for different values of N_x and M_t. The efficiency and accuracy of the new scheme have been verified using the results provided in Table 1. From the orders of convergence provided in these tables, the proposed numerical method is shown to be second-order accurate in both directions. The CPU time is also presented in this table, which reveals that the time taken to solve the problem using the proposed scheme is much less. Also, the relative error measures for various values of x and t are shown in Table 2.

To explore the behavior of the solution to the problem, a surface plot of the approximate solution was constructed and is provided in Figure 1(a). In addition, the approximation of the solution at different time levels is provided in Figure 1(b). A comparison between the numerical and the exact solution is presented in Figure 2 accompanied by the corresponding error measures; this shows that the approximate solution is quite near to the actual solution.

Table 1. Errors in L_2-norm and orders of convergence, with CPU time in seconds, for Example 5.1.

	Number of nodal points				
α	16	32	64	128	256
0.1	$2.09E-03$	$5.22E-04$	$1.31E-04$	$3.26E-05$	$8.16E-06$
	2.0014	1.9945	2.0066	1.9982	
0.3	$2.04E-03$	$5.09E-04$	$1.28E-04$	$3.19E-05$	$7.99E-06$
	2.0028	1.9915	2.0045	1.9973	
0.5	$1.96E-03$	$4.93E-04$	$1.24E-04$	$3.10E-05$	$7.76E-06$
	1.9912	1.9912	2.0000	1.9981	
0.7	$2.36E-03$	$6.11E-04$	$1.56E-04$	$3.92E-05$	$9.86E-06$
	1.9495	1.9696	1.9926	1.9912	
0.9	$2.24E-01$	$7.84E-02$	$2.22E-02$	$5.85E-03$	$1.50E-03$
	1.5146	1.8203	1.9241	1.9635	
CPU-time	0.0291	0.0483	0.0996	0.6540	1.1752

Table 2. Relative errors at different values of x and t, $\alpha = 0.3$ and $M = N = 64$ for Example 5.1.

	t			
x	0.2	0.4	0.6	0.8
0.1	$8.9306E-05$	$1.7975E-04$	$2.0089E-04$	$2.0906E-04$
0.2	$6.2970E-05$	$1.6102E-04$	$1.8394E-04$	$1.9278E-04$
0.4	$3.6918E-05$	$1.4247E-04$	$1.6713E-04$	$1.7664E-04$
0.6	$1.0185E-05$	$1.2342E-04$	$1.4987E-04$	$1.6006E-04$
0.8	$1.8108E-05$	$1.0327E-04$	$1.3161E-04$	$1.4253E-04$
0.9	$5.4037E-05$	$7.7708E-05$	$1.0845E-04$	$1.2030E-04$

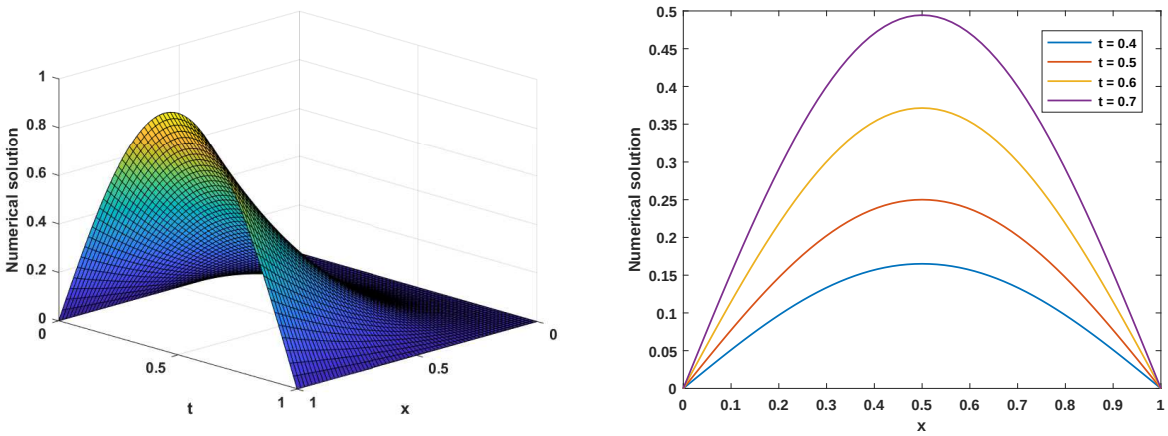

(a) (b)

Figure 1. Numerical solution for Example 5.1 for $\alpha = 0.4$.

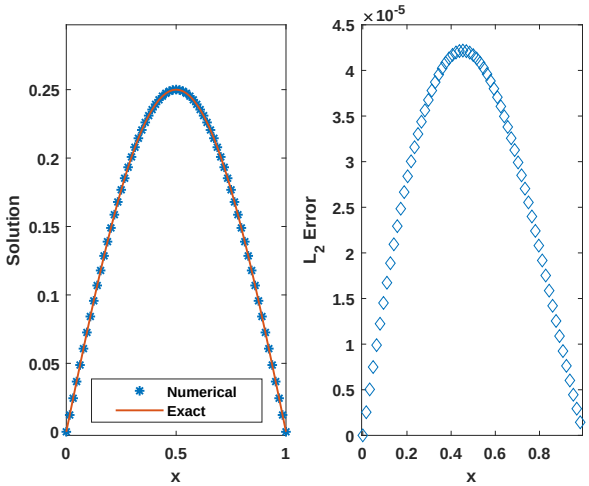

Figure 2. Comparison of the exact and numerical solutions for Example 5.1 at $t = 0.5$ and given $\alpha = 0.4$.

Example 5.1. *Consider the problem described by Eq (3.1) with* $\nu = \rho = 1$. *In addition, the initial and boundary conditions and the source term are calculated using the exact solution of the model given by* $u = sin(\pi x)t^2$.

Example 5.2. *Consider the problem described by Eq (3.1) with* $\nu = 2$ *and* $\rho = 3$. *In addition, the initial and boundary conditions and the source term are calculated using the exact solution of the model given by* $u = x^2(x^3 - \frac{5}{2}x^2 + 2x - \frac{1}{2})t^4$.

Let us look at another example to support the accuracy of the above-mentioned findings and observations. In this case, we also considered an example for which the exact answer is known solely to ensure the algorithm's accuracy. Tables and graphs are used to illustrate the numerical results. In this

context, Figure 3(a) is the graphical representation of the approximate solution for $\alpha = 0.8$. However, Figure 3(b) represents the variation in the behavior of the numerical solution with varying t, and for a fixed $\alpha = 0.8$. In addition, Figure 4 shows a comparison of the approximate and actual solutions at $t = 0.5$ given $\alpha = 0.8$ and the corresponding error measures; moreover, the figure presents the accuracy of the numerical algorithm graphically. Next, Table 3 summarizes the error that occurred while computing the solution to Example 5.2 numerically for various values of α. The orders of convergence for each value of α, along with the CPU time taken to calculate the solution, are also given. Table 4 contains the relative error measures for different values of x and t. These tabulated results indicate that the proposed scheme is accurate and can be used to solve fractional Partial Differential Equations (PDEs) arising in different areas efficiently.

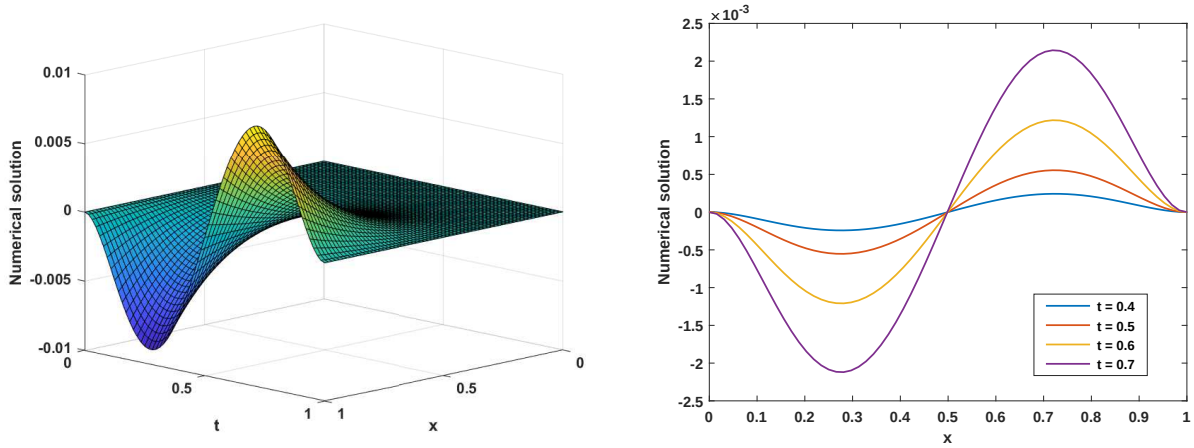

(a) (b)

Figure 3. Numerical solution for Example 5.2 for $\alpha = 0.8$.

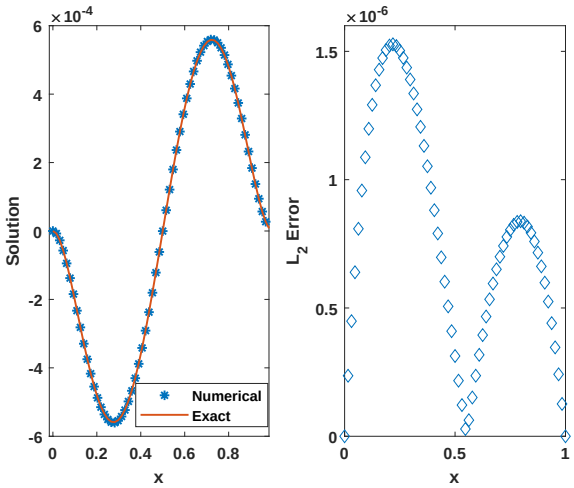

Figure 4. Comparison of the exact and numerical solutions to Example 5.2 at $t = 0.5$, and for $\alpha = 0.8$.

Table 3. Errors in L_2-norm and orders of convergence, with CPU time in seconds, for Example 5.2.

	Number of nodal points				
α	16	32	64	128	256
0.1	$2.31E-04$	$5.79E-05$	$1.45E-05$	$3.62E-06$	$9.06E-07$
	1.9963	1.9975	2.0020	1.9984	
0.3	$2.30E-04$	$5.78E-05$	$1.45E-05$	$3.61E-06$	$9.04E-07$
	1.9925	1.9950	2.0060	1.9976	
0.5	$2.29E-04$	$5.75E-05$	$1.44E-05$	$3.60E-06$	$8.99E-07$
	1.9937	1.9975	2.0000	2.0016	
0.7	$2.27E-04$	$5.68E-05$	$1.42E-05$	$3.56E-06$	$8.90E-07$
	1.9987	2.0000	1.9959	2.0000	
0.9	$1.90E-04$	$5.10E-05$	$1.32E-05$	$3.37E-06$	$8.51E-07$
	1.8974	1.9500	1.9697	1.9855	
CPU-time	0.0331	0.0483	0.0986	0.3990	1.0162

Table 4. Relative errors at different values of x and t, $\alpha = 0.5$ and $M = N = 64$ for Example 5.2.

	t			
x	0.2	0.4	0.6	0.8
0.1	$3.2653E-02$	$3.2896E-02$	$3.2955E-02$	$3.2979E-02$
0.2	$3.0812E-03$	$3.1257E-03$	$3.1365E-03$	$3.1408E-03$
0.4	$2.5169E-03$	$2.5758E-03$	$2.5903E-03$	$2.5964E-03$
0.6	$8.0655E-04$	$8.1806E-04$	$8.1993E-04$	$8.2025E-04$
0.8	$1.6893E-03$	$1.7200E-03$	$1.7267E-03$	$1.7291E-03$
0.9	$1.7331E-02$	$1.7562E-02$	$1.7613E-02$	$1.7632E-02$

In the next example, we include a reaction term in the advection dispersion equation; thus, the equation is termed as a time-fractional advection-dispersion-reaction equation, which has been widely studied for the solute transport processes [26]. The equation is given by

$$ {}_{0}^{MABC}D_t^{\alpha}u = \nu\frac{\partial^2 u}{\partial x^2} - \rho\frac{\partial u}{\partial x} + \kappa u + f(x,t), \quad 0 < x < 1, \quad 0 < t \leq 1. \tag{5.1} $$

Example 5.3. *Consider the problem described by Eq (5.1) with $\nu = 1$, $\rho = 3$ and $\kappa = 2$. In addition, the initial and boundary conditions and the source term are calculated using the exact solution of the model given by $u = x(x-1)t^2$.*

This example also shows the viability of the scheme, as can be confirmed by the numerical results that we have illustrated in Tables 5 and 6. Figure 5(a) presents the graph of the approximate solution and Figure 5(b) displays the numerical solution at distinct time levels for $\alpha = 0.8$. In addition Figure 6 shows a comparison of the approximate and actual solutions at $t = 0.5$ given $\alpha = 0.4$ and the

corresponding error measures; moreover, the figure presents the accuracy of the numerical algorithm graphically. The orders of convergence for each value of α along with the CPU time taken to calculate the solution are also given. The plots and tabulated results show the efficiency of the scheme, which can be applied to a variety of time-fractional PDEs.

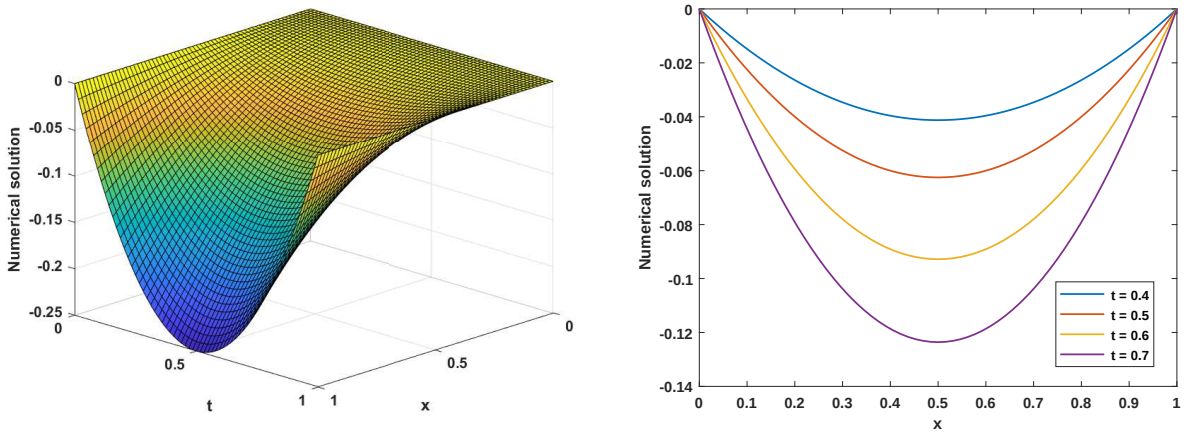

(a) (b)

Figure 5. Numerical solution for Example 5.3 for $\alpha = 0.8$.

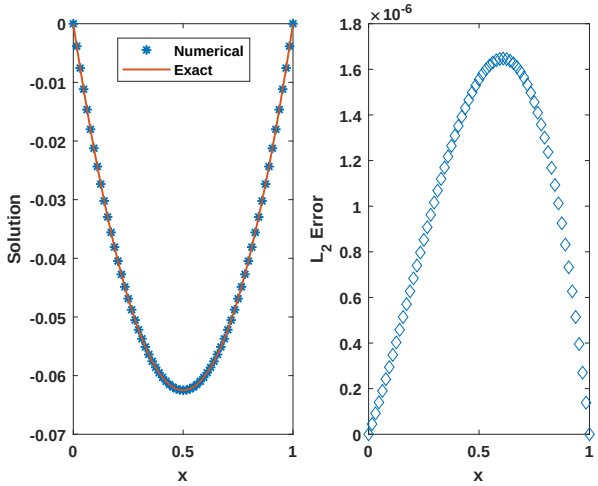

Figure 6. Comparison of the exact and numerical solutions to Example 5.3 at $t = 0.5$, and for $\alpha = 0.4$.

Table 5. Errors in L_2-norm and orders of convergence, with CPU time in seconds, for Example 5.3.

	Number of nodal points				
α	16	32	64	128	256
0.1	$6.13E-06$	$1.47E-06$	$3.55E-07$	$8.59E-08$	$2.08E-08$
	2.0601	2.0499	2.0471	2.0461	
0.3	$1.73E-05$	$4.04E-06$	$9.49E-07$	$2.25E-07$	$5.36E-08$
	2.0983	2.0899	2.0765	2.0696	
0.5	$2.90E-05$	$6.61E-06$	$1.54E-06$	$3.65E-07$	$8.76E-08$
	2.1333	2.1017	2.0770	2.0589	
0.7	$1.47E-04$	$4.03E-05$	$1.09E-05$	$2.81E-06$	$7.16E-07$
	1.8670	1.8865	1.9557	1.9725	
0.9	$8.35E-02$	$2.22E-02$	$6.26E-03$	$1.65E-03$	$4.23E-04$
	1.9112	1.8263	1.9237	1.9637	
CPU-time	0.0401	0.0642	0.0992	0.42901	1.1769

Table 6. Relative errors at different values of x and t, $\alpha = 0.4$ and $M = N = 64$ for Example 5.3.

	t			
x	0.2	0.4	0.6	0.8
0.1	$5.8680E-05$	$1.7008E-05$	$1.1440E-07$	$4.9160E-06$
0.2	$8.4919E-05$	$2.4622E-05$	$1.1749E-05$	$7.1190E-06$
0.4	$1.1261E-04$	$3.2670E-05$	$1.5595E-05$	$9.4510E-06$
0.6	$1.3892E-04$	$4.0327E-05$	$1.9257E-05$	$1.1672E-05$
0.8	$1.6122E-04$	$4.6819E-05$	$2.2362E-05$	$1.3556E-05$
0.9	$1.8057E-04$	$5.2448E-05$	$2.5053E-05$	$1.5189E-05$

6. Conclusions

In this paper, we have developed a novel approximation method for the MABC derivative of the fractional-order α of a function $f(t) \in L^1(0,1)$. Further, the numerical estimation of the MABC derivative has been used to solve a time-fractional advection-dispersion equation. The proposed numerical scheme is proficient and gives the second-order of accuracy in both the temporal and spatial directions. Moreover, using Fourier analysis it has been proved that the scheme is unconditionally stable. Furthermore, two test problems were solved to validate the theoretical findings. The tabulated results and numerical plots show that the solution obtained by using the proposed numerical technique is completely concordant with the exact solution. Regarding the application, one can apply the present numerical approach to a wide range of problems defined in terms of MABC derivatives encountered in science and technology.

Acknowledgments

The authors present their sincere gratitude to the unknown reviewers for many valuable comments and corrections. The second author is grateful to Council of Scientific and Industrial Research (CSIR), New Delhi, India (award letter No. 09/719(0096)/2019-EMR-I).

Conflict of interest

The authors state that they have no known competing financial interests or personal ties that could have influenced the research presented in this study.

References

1. A. A. Kilbas, H. M. Srivastava, J. J. Trujillo, *Theory and applications of fractional differential equations*, Amsterdam: Elsevier, 2006.
2. I. Podlubny, *Fractional differential equations*, San Diego: Academic Press, 1999.
3. H. Scher, E. W. Montroll, Anomalous transit-time dispersion in amorphous solids, *Phys. Rev. B*, **12** (1975), 2455–2477. https://doi.org/10.1103/PhysRevB.12.2455
4. I. M. Sokolov, J. Klafter, A. Blumen, Ballistic versus diffusive pair-dispersion in the Richardson regime, *Phys. Rev. E*, **61** (2000), 2717–2722. https://doi.org/10.1103/PhysRevE.61.2717
5. T. L. Szabo, J. Wu, A model for longitudinal and shear wave propagation in viscoelastic media, *J. Acoust. Soc. Am.*, **107** (2000), 2437–2446. https://doi.org/10.1121/1.428630
6. R. Hilfer, *Applications of fractional calculus in physics*, Singapore: World Scientific, 2000. https://doi.org/10.1142/3779
7. Z. Liu, X. Li, A Crank-Nicolson difference scheme for the time variable fractional mobile-immobile advection-dispersion equation, *J. Appl. Math. Comput.*, **56** (2018), 391–410. https://doi.org/10.1007/s12190-016-1079-7
8. M. M. Meerschaert, C. Tadjeran, Finite difference approximations for fractional advection-dispersion flow equations, *J. Comput. Appl. Math.*, **172** (2004), 65–77. https://doi.org/10.1016/j.cam.2004.01.033
9. M. M. Meerschaert, C. Tadjeran, Finite difference approximations for two-sided space-fractional partial differential equations, *Appl. Numer. Math.*, **56** (2006), 80–90. https://doi.org/10.1016/j.apnum.2005.02.008
10. M. Yaseen, M. Abbas, A. I. Ismail, T. Nazir, A cubic trigonometric B-spline collocation approach for the fractional sub-diffusion equations, *Appl. Math. Comput.*, **293** (2017), 311–319. https://doi.org/10.1016/j.amc.2016.08.028
11. M. Stynes, Singularities, In: *Handbook of fractional calculus with applications, Volume 3*, Walter de Gruyter GmbH, 2019, 287–305. https://doi.org/10.1515/9783110571684-011
12. M. Caputo, M. Fabrizio, A new definition of fractional derivative without singular kernel, *Progr. Fract. Differ. Appl.*, **1** (2015), 73–85. http://doi.org/10.12785/pfda/010201
13. D. Baleanu, A. Mousalou, S. Rezapour, A new method for investigating approximate solutions of some fractional integro-differential equations involving the Caputo–Fabrizio derivative, *Adv. Differ. Equ.*, **2017** (2017), 51. https://doi.org/10.1186/s13662-017-1088-3

14. Z. Liu, A. J. Cheng, X. Li, A second order finite difference scheme for quasilinear time fractional parabolic equation based on new fractional derivative, *Int. J. Comput. Math.*, **95** (2018), 396–411. https://doi.org/10.1080/00207160.2017.1290434
15. M. Zhang, Y. Liu, H. Li, High-order local discontinuous Galerkin method for a fractal mobile/immobile transport equation with the Caputo-Fabrizio fractional derivative, *Numer. Method. Part. Differ. Equ.*, **35** (2019), 1588–1612. https://doi.org/10.1002/num.22366
16. A. Atangana, D. Baleanu, New fractional derivatives with non-local and non-singular kernel: theory and application to heat transfer model, *Therm. Sci.*, **20** (2016), 763–769. https://doi.org/10.2298/TSCI160111018A
17. N. Sene, K. Abdelmalek, Analysis of the fractional diffusion equations described by Atangana-Baleanu-Caputo fractional derivative, *Chaos Soliton. Fract.*, **127** (2019), 158–164. https://doi.org/10.1016/j.chaos.2019.06.036
18. M. Shafiq, M. Abbas, K. M. Abualnaja, M. J. Huntul, A. Majeed, T. Nazir, An efficient technique based on cubic B-spline functions for solving time-fractional advection diffusion equation involving Atangana-Baleanu derivative, *Eng. Comput.*, **38** (2022), 901–917. https://doi.org/10.1007/s00366-021-01490-9
19. H. Tajadodi, A Numerical approach of fractional advection-diffusion equation with Atangana-Baleanu derivative, *Chaos Soliton. Fract.*, **130** (2020), 109527. https://doi.org/10.1016/j.chaos.2019.109527
20. M. A. Refai, D. Baleanu, On an extension of the operator with mittag-leffler kernel, *Fractals*, in press. https://doi.org/10.1142/S0218348X22401296
21. F. Liu, P. Zhuang, K. Burrage, Numerical methods and analysis for a class of fractional advection-dispersion models, *Comput. Math. Appl.*, **64** (2012), 2990–3007. https://doi.org/10.1016/j.camwa.2012.01.020
22. M. K. Singh, A. Chatterjee, V. P. Singh, Solution of one-dimensional time fractional advection dispersion equation by homotopy analysis method, *J. Eng. Mech.*, **143** (2017), 04017103. https://doi.org/10.1061/(ASCE)EM.1943-7889.0001318
23. Y. Zhang, D. A. Benson, D. M. Reeves, Time and space nonlocalities underlying fractional-derivative models: Distinction and literature review of field applications, *Adv. Water Resour.*, **32** (2009), 561–581. https://doi.org/10.1016/j.advwatres.2009.01.008
24. K. Miller, B. Ross, *An introduction to the fractional calculus and fractional differential equations*, New York: Wiley, 1993.
25. K. B. Oldham, J. Spanier, *The fractional calculus*, New York: Academic Press, 1974.
26. A. Jannelli, M. Ruggieri, M. P. Speciale, Analytical and numerical solutions of time and space fractional advection-diffusion-reaction equation, *Commun. Nonlinear Sci. Numer. Simul.*, **70** (2019), 89–101. https://doi.org/10.1016/j.cnsns.2018.10.012

AIMS Press